

Bio-based Renewable Additives for Anti-icing Applications (Phase I)



Mehdi Honarvar Nazari, Eden Adele Havens, Xianming Shi
Department of Civil & Environmental Engineering
Washington State University

Anburaj Muthumani
Western Transportation Institute
Montana State University

Date: 09/04/2016

Prepared by:

Center for Environmentally Sustainable
Transportation in Cold Climates
Duckering Building, Room 245
P.O. Box 755900
Fairbanks, AK 99775

U.S. Department of Transportation
1200 New Jersey Avenue, SE
Washington, DC 20590

INE/CESTiCC 101406



REPORT DOCUMENTATION PAGE			Form approved OMB No.
Public reporting for this collection of information is estimated to average 1 hour per response, including the time for reviewing instructions, searching existing data sources, gathering and maintaining the data needed, and completing and reviewing the collection of information. Send comments regarding this burden estimate or any other aspect of this collection of information, including suggestion for reducing this burden to Washington Headquarters Services, Directorate for Information Operations and Reports, 1215 Jefferson Davis Highway, Suite 1204, Arlington, VA 22202-4302, and to the Office of Management and Budget, Paperwork Reduction Project (0704-1833), Washington, DC 20503			
1. AGENCY USE ONLY (LEAVE BLANK)	2. REPORT DATE 03/2016	3. REPORT TYPE AND DATES COVERED Final Report: 9/2014 – 12/2015	
4. TITLE AND SUBTITLE Bio-based Renewable Additives for Anti-icing Applications (Phase I)			5. FUNDING NUMBERS
6. AUTHOR(S) Honarvar Nazari, Mehdi, Ph.D. in Metallurgical and Materials Engineering Graduate Research Assistant, Department of Civil & Environmental Engineering, P.O. Box 642910, Washington State University, Pullman, WA 99164-2910 Havens, Eden Adele, Undergraduate Research Assistant Department of Civil & Environmental Engineering, P.O. Box 642910, Washington State University, Pullman, WA 99164-2910 Muthumani, Anburaj, Research Engineer Winter Maintenance & Effects Program, Western Transportation Institute, Montana State University, P.O. Box 174250, Bozeman, MT 59717 Shi, Xianming, Ph.D., P.E., Associate Professor Director of Laboratory of Corrosion Science & Electrochemical Engineering, Department of Civil & Environmental Engineering, P.O. Box 642910, Washington State University, Pullman, WA 99164-2910			
7. PERFORMING ORGANIZATION NAME(S) AND ADDRESS(ES) Center for Environmentally Sustainable Transportation in Cold Climates University of Alaska Fairbanks Duckering Building, Room 245 P.O. Box 755900 Fairbanks, AK 99775-5900			8. PERFORMING ORGANIZATION REPORT NUMBER
9. SPONSORING/MONITORING AGENCY NAME(S) AND ADDRESS(ES) U.S. Department of Transportation 1200 New Jersey Avenue, SE Washington, DC 20590			10. SPONSORING/MONITORING AGENCY REPORT NUMBER
11. SUPPLEMENTARY NOTES			
12a. DISTRIBUTION / AVAILABILITY STATEMENT: No restrictions			12b. DISTRIBUTION CODE
13. ABSTRACT: The performance and impacts of several bio-based anti-icers along with a traditional chloride-based anti-icer (salt brine) were evaluated. A statistical design of experiments (uniform design) was employed for developing anti-icing liquids consisting of cost-competitive chemicals such as bio-based compounds (e.g., sugar beet extract and dandelion extract), rock salt, sodium metasilicate, and sodium formate. The following experimentally obtained parameters were examined as a function of the formulation design: ice-melting capacity and ice penetration at 25°F (-3.9°C) and 15°F (-9.4°C), compressive strength of Portland cement mortar samples after 10 freeze-thaw/deicer cycles, corrosion rate of C1010 carbon steel after 24-hour immersion, and impact on asphalt binder's stiffness. One viable formula ("best performer") was tested for freezing point depression phase diagram (ASTM D1177-88) and the friction coefficient of asphalt pavement treated by this anti-icing formulation (vs. 23 wt.% NaCl) at a certain temperature near 25°F or 30°F after being applied at 30 gallons per lane mile (1 hour after simulated trafficking and plowing). Laboratory data shed light on the selection and formulation of innovative bio-based snow and ice control chemicals that can significantly reduce the costs of winter maintenance operations. This exploratory investigation contributes to more systematic study of optimizing "greener" anti-icers using renewable resources.			
14. KEYWORDS: Bio-based anti-icer; ice-melting performance; Portland cement mortar; compressive strength; asphalt binder; stiffness; m-value; corrosivity; freezing point depression; friction coefficient			15. NUMBER OF PAGES: 30
			16. PRICE CODE: N/A
17. SECURITY CLASSIFICATION OF REPORT Unclassified	18. SECURITY CLASSIFICATION OF THIS PAGE Unclassified	19. SECURITY CLASSIFICATION OF ABSTRACT Unclassified	20. LIMITATION OF ABSTRACT N/A

Bio-based Renewable Additives for Anti-icing Applications (Phase I)

Mehdi Honarvar Nazari, Ph.D.

Ph.D. in Metallurgical and Materials Engineering
Graduate Research Assistant, Smart and Green Infrastructure Group
Department of Civil & Environmental Engineering
P.O. Box 642910, Washington State University
Pullman, WA 99164-2910
(626) 375-1992 phone; (509) 335-7632 fax
Email: m.honarvarnazari@wsu.edu

Eden Adele Havens

Undergraduate Research Assistant, Smart and Green Infrastructure Group
Department of Civil & Environmental Engineering
P.O. Box 642910, Washington State University
Pullman, WA 99164-2910
(253) 327-9978 phone; (509) 335-7632 fax
Email: eden.havens@wsu.edu

Anburaj Muthumani, M. Sc., P.E.

Research Engineer, Winter Maintenance & Effects Program
Western Transportation Institute, Montana State University
P.O. Box 174250, Bozeman, MT 59717
Phone: (406) 994-6782; Fax: (406) 994-1697
Email: anburaj.muthumani@montana.edu

Xianming Shi, Ph.D., P.E.*

Associate Professor and Director, Laboratory of Corrosion Science & Electrochemical Engineering (CSEE)
Department of Civil & Environmental Engineering
Washington State University
P.O. Box 642910
Pullman, WA 99164-2910
(509) 335-7088 phone; (509) 335-7632 fax
Email: xianming.shi@wsu.edu

* Principal Investigator

Prepared by:

Center for Environmentally Sustainable
Transportation in Cold Climates
Duckering Building, Room 245
P.O. Box 755900
Fairbanks, AK 99775

U.S. Department of Transportation
1200 New Jersey Avenue, SE
Washington, DC 20590

Date: 09/04/2016

INE/CESTiCC 101406

DISCLAIMER

This document is disseminated under the sponsorship of the U.S. Department of Transportation in the interest of information exchange. The U.S. Government assumes no liability for the use of the information contained in this document. The U.S. Government does not endorse products or manufacturers. Trademarks or manufacturers' names appear in this report only because they are considered essential to the objective of the document. Opinions and conclusions expressed or implied in the report are those of the author(s). They are not necessarily those of the funding agencies.

METRIC (SI*) CONVERSION FACTORS

APPROXIMATE CONVERSIONS TO SI UNITS					APPROXIMATE CONVERSIONS FROM SI UNITS				
Symbol	When You Know	Multiply By	To Find	Symbol	Symbol	When You Know	Multiply	To Find	Symbol
<u>LENGTH</u>					<u>LENGTH</u>				
in	inches	25.4		mm	mm	millimeters	0.039	inches	in
ft	feet	0.3048		m	m	meters	3.28	feet	ft
yd	yards	0.914		m	m	meters	1.09	yards	yd
mi	Miles (statute)	1.61		km	km	kilometers	0.621	Miles (statute)	mi
<u>AREA</u>					<u>AREA</u>				
in ²	square inches	645.2	millimeters squared	cm ²	mm ²	millimeters squared	0.0016	square inches	in ² m ²
ft ²	square feet	0.0929	meters squared	m ²	meters squared	10.764	square feet	ft ²	
yd ²	square yards	0.836	meters squared	m ²	m ²	meters squared	1.196	square yards	yd ²
mi ²	square miles	2.59	kilometers squared	km ²	km ²	kilometers squared	0.39	square miles	mi ² ha
ac	acres	0.4046	hectares	ha	hectares (10,000 m ²)	2.471	acres	ac	
<u>MASS (weight)</u>					<u>MASS (weight)</u>				
oz	Ounces (avdp)	28.35	grams	g	g	grams	0.0353	Ounces (avdp)	oz
lb	Pounds (avdp)	0.454	kilograms	kg	kg	kilograms	2.205	Pounds (avdp)	lb mg
T	Short tons (2000 lb)	0.907	megagrams	mg	megagrams (1000 kg)	1.103	short tons	T	
<u>VOLUME</u>					<u>VOLUME</u>				
fl oz	fluid ounces (US)	29.57	milliliters	mL	mL	milliliters	0.034	fluid ounces (US)	fl oz
gal	Gallons (liq)	3.785	liters	liters	liters	liters	0.264	Gallons (liq)	gal
ft ³	cubic feet	0.0283	meters cubed	m ³	m ³	meters cubed	35.315	cubic feet	ft ³
yd ³	cubic yards	0.765	meters cubed	m ³	m ³	meters cubed	1.308	cubic yards	yd ³
Note: Volumes greater than 1000 L shall be shown in m ³									
<u>TEMPERATURE (exact)</u>					<u>TEMPERATURE (exact)</u>				
°F	Fahrenheit temperature	5/9 (°F-32)	Celsius temperature	°C	°C	Celsius temperature	9/5 °C+32	Fahrenheit temperature	°F
FORCE and PRESSURE or STRESS					FORCE and PRESSURE or STRESS				
lbf	pound-force	4.45	newtons	N	N	newtons	0.225	pound-force	lbf
psi	pound-force per square inch	6.89	kilopascals	kPa	kPa	kilopascals	0.145	pound-force per square inch	psi
These factors conform to the requirement of FHWA Order 5190.1A *SI is the symbol for the International System of Measurements									

ACKNOWLEDGMENTS

The authors acknowledge the financial support provided by the Center for Environmentally Sustainable Transportation in Cold Climates (CESTiCC), Laura Fay at Western Transportation Institute – Montana State University for providing lab access to run complementary tests, and the Washington State Department of Transportation for providing rock salt.

Table of Contents

Disclaimer	i
Acknowledgments	i
List of Figures	iv
List of Tables	v
Executive Summary	vi
Abstract	viii
CHAPTER 1.0 INTRODUCTION	1
1.1 Problem Statement	1
1.2 Background	1
1.3 Objectives	2
1.4 Expected Benefits	3
CHAPTER 2.0 METHODOLOGY	4
2.1 Research Approach	4
2.2 Work Plan – Task Descriptions and Milestones	4
2.2.1 Identify and Evaluate Individual “Green” Additives	4
2.2.2 Statistical Design of Experiments	5
2.2.3 Systematic Laboratory Investigation and Formulation Optimization	5
Preparation of the plant extract	6
Freeze-thaw test	7
Ice-melting test	8
Low-temperature behavior of asphalt binder	8
Ice-penetration test	9
Corrosion behavior	9
Eutectic curves	10
Chemical analysis	10
Friction test	11
CHAPTER 3.0 RESULTS AND DISCUSSION	13
3.1 Ice-Melting Capacity of Anti-icers	13
3.2 Freeze-Thaw Resistance of PCM in the Presence of Anti-icers	13
3.3 Effect of Freeze-Thaw in the Presence of Anti-icers on the PCM Strength	14
3.4 Impacts of Anti-icer Mixtures on Asphalt Pavements	15
3.5 The Corrosivity of Anti-icer Mixtures on Mild Steel	16
3.6 FTIR Spectroscopy of Sugar Beet By-product	17

3.7 Liquid Chromatography–Mass Spectrometry	19
3.8 Complementary Tests	20
3.8.1 Ice-Melting Capacity of Selected Anti-icers	21
3.8.2 Ice-Penetration Rate of Selected Anti-icers	21
3.8.3 Eutectic and Effective Temperatures	23
3.8.4 Friction Coefficient of Anti-iced Pavement Surface	24
CHAPTER 4.0 CONCLUSIONS AND RECOMMENDATIONS	26
CHAPTER 5.0 REFERENCES	28
APPENDIX A	31

List of Figures

Figure 1.1 Sugar beets (left) and their harvesting in Montana (right) (Courtesy: Montankids.com and BillingsGazette.com).....	3
Figure 3.1 Ranking of mixtures based on ice-melting capacity after application of anti-icers at 60 min, 15°F obtained using a SHRP test method.....	13
Figure 3.2 Weight loss of Portland cement mortars exposed to various anti-deicer mixtures after the 10-day SHRP H205.8 freeze-thaw test.....	14
Figure 3.3 Compressive strength of mortar as a function of anti-icer type after 10-cycle freeze-thaw test.	15
Figure 3.4 The stiffness of asphalt binder exposed to various anti-icer mixtures obtained by a BBR.....	16
Figure 3.5 The <i>m</i> -value of asphalt binder exposed to various anti-icer mixtures obtained by a BBR.....	16
Figure 3.6 Corrosivity of the anti-icer mixtures on C1010 carbon steel after 24 h immersion measured by LPR.....	18
Figure 3.7 FTIR spectra for sugar beet by-product.....	19
Figure 3.8 LC–MS spectra of sugar beet extract.	20
Figure 3.9 Ice-melting capacity as a function of time at 25°F obtained using the SHRP test method.....	22
Figure 3.10 Ice-melting capacity as a function of time at 15°F obtained using the SHRP test method.....	22
Figure 3.11 Ice-penetration rate as a function of time at 25°F obtained using the SHRP test method.....	23
Figure 3.12 Ice-penetration rate as a function of time at 15°F obtained using the SHRP test method.....	23
Figure 3.13 Eutectic curves of salt brine and Mix 1.	24
Figure 3.14 Friction coefficient on the iced asphalt pavement at about 25°F in the absence of anti-icer and after application of salt brine and Mix 1 as anti-icers.	25

List of Tables

Table 2.1 Experimental design for anti-icer mixtures based on uniform design method.	6
Table 3.1 Chemical functional groups of the sugar beet by-product obtained using FTIR spectroscopy.....	19
Table 3.2 Summary of the chemical constituents detected for sugar beet by-product using the liquid chromatography–mass spectrometry (LC-MS) technique.....	20

Executive Summary

Road maintenance agencies are continually challenged in providing a high level of service on roadways and improving safety and mobility in a cost-effective manner while minimizing adverse effects to the environment. Large amounts of liquid chemicals, known as anti-icers, are applied on roadways during winter to keep them clear of ice and snow. These anti-icers are mainly chloride-based salts that do not degrade once used and thus pose significant environmental risk over time. About 20 million tons of chloride-based salts are used annually in the United States for snow and ice control purposes. Maintenance agencies are constantly seeking an alternative to chloride-based deicing salts with maximum anti-icing efficiency and minimum drawback.

In recent decades, agro-based chemicals such as desugared beet molasses and glycerol have been introduced in snow and ice control operations, used alone or more commonly used as additives for chloride-based products. Agro-based chemicals are produced by fermentation and processing of beet juice, molasses, corn, and other agricultural products. The deicer formulation is noncorrosive, inexpensive, water soluble, and readily available in large quantities. Agro-based additives provide enhanced ice-melting capacity, reduce deicer corrosivity, and remain effective on roadways longer than standard chemicals.

Through this project, the research team has developed an innovative high-performance “green” anti-icer that can minimize the impacts of traditional chloride-based salts on concrete, asphalt, and metallic components. Selected constituent materials in this anti-icer pose minimal toxicity to the environment (e.g., no heavy metal contents) and are derived from eco-friendly cost-effective processes. Bio-based solutions derived from locally sourced agro-based materials mixed with 23 wt.% salt brine and commercial additives (with little toxicity) have been tested for ice-melting capacity, ice-penetration rate, ability to protect asphalt binder and concrete, effect on the

friction coefficient of iced asphalt pavement, and anti-corrosion performance. In this research, a 23 wt.% salt brine was considered the control. The main criteria for choosing the best performing anti-icer were ice-melting capacity and capability to increase the friction coefficient of iced asphalt pavement.

This research contributes to the knowledge base relevant to bio-based anti-icers and introduces a new class of high-performance “green” anti-icers. Before scale-up production of these materials, more research to optimize the formula and field validation of its performance is needed. Future research could include the exploration of other types of “green” anti-icers consisting of additives derived from renewable resources other than sugar beet.

Abstract

The performance and impacts of several bio-based anti-icers along with a traditional chloride-based anti-icer (salt brine) were evaluated. A statistical design of experiments (uniform design) was employed for developing anti-icing liquids consisting of cost-competitive chemicals such as bio-based compounds (e.g., sugar beet extract and dandelion extract), rock salt, sodium metasilicate, and sodium formate. The following experimentally obtained parameters were examined as a function of the formulation design: ice-melting capacity and ice penetration at 25°F (-3.9°C) and 15°F (-9.4°C), compressive strength of Portland cement mortar (PCM) samples after 10 freeze-thaw/deicer cycles, the corrosivity of C1010 carbon steel after 24-hour immersion, and impact on asphalt binder stiffness. One viable formula (“best performer”) was tested for freezing point depression phase diagram (ASTM D1177-88) and the friction coefficient of asphalt pavement treated by the anti-icing formulation (vs. 23 wt.% NaCl) at a certain temperature near 25°F or 30°F after being applied at 30 gallons per lane mile (1 hour after simulated trafficking and plowing). Laboratory data shed light on the selection and formulation of innovative bio-based snow and ice control chemicals that can significantly reduce the costs of winter maintenance operations. This exploratory investigation contributes to more systematic study of optimizing “greener” anti-icers using renewable resources.

Keywords: Bio-based anti-icer; ice-melting performance; Portland cement mortar; compressive strength; asphalt binder; stiffness; m-value; corrosivity; freezing point depression; friction coefficient

CHAPTER 1.0 INTRODUCTION

1.1 Problem Statement

It has become increasingly clear that the environmental cost associated with using snow and ice control products must be balanced with the value they provide. In this context, sustainability principles are needed in the winter maintenance of highways. Relative to deicing and sanding, anti-icing leads to improved level of service, reduced need for chemicals, associated cost savings, and safety and mobility benefits (Conger, 2005; Staples et al., 2004). Yet, concerns are growing over the anti-icers available on the market and their corrosion to metals (chlorides), impact on concrete and asphalt (acetates), toxicity to the aquatic resources (oxygen depletion), etc. Agencies are constantly seeking alternatives that will maximize the benefits of acetates and agro-based products while minimizing their drawbacks. Meanwhile, research is needed on the value-added utilization of desugared beet molasses and glycerol, the principal by-products of beet sugar refining and biodiesel production, respectively.

1.2 Background

Currently, the United States spends approximately \$2.3 billion annually to keep highways free of snow and ice; the associated corrosion and environmental impacts add at least \$5 billion (Fay et al., 2013). Agencies are continually challenged to ensure safe, reliable winter highways in a cost-effective and eco-friendly manner, while dealing with increased traffic demands, higher customer expectations, and unprecedented staffing and funding constraints (Fay et al., 2013; Li et al., 2013; Shi et al., 2013). In a previous study by Ye et al. (2009), winter maintenance operations of the Nevada Department of Transportation (NDOT) were examined. Ye et al. found that NDOT spent approximately \$12.8 million on road maintenance operations during winter season 2006–07. They also found that use of better weather information led to tangible benefits of about \$0.6 million per season, as it enabled more proactive strategies for

snow and ice control. In other words, better practices have great potential to significantly reduce the cost of winter maintenance operations.

Chloride salts do not degrade once released to the environment; they thus pose a significant environmental risk over time (Fay et al., 2014). Currently about 20 million tons of sodium chloride salts are used for snow and ice control on highways and other roadways in the United States each year (Kelly et al., 2010). Glycerol, a by-product of biodiesel or triglyceride processing, was disclosed as a key ingredient for anti-icing or deicing fluids in at least two patents (Sapienza et al., 2005, 2012). The brines made of glycerol, sodium chloride (NaCl), magnesium chloride (MgCl₂), and commercial deicers, individually or in combination, were evaluated by Taylor et al. (2010), who concluded that a blend of 80% glycerol with 20% NaCl shows the greatest promise in good performance and low negative impacts. This blend, however, is highly viscous. Dilution of the blend allows anti-icing application, but can undermine the blend's effectiveness. Furthermore, the use of glycerol may pose a potential risk to water quality, which has to be mitigated by limiting the amount of glycerol in the formulation to control its contaminants. Glycerol merits more research to explore the synergy of it and other additives in optimizing liquid product formulations. Desugared molasses, a by-product of the beet sugar refining process, is readily available at low cost and has been disclosed as an effective user-friendly and environmentally friendly ingredient for anti-icing, deicing, or pre-wetting operations (Bloomer, 2002; Ossian and Behrens, 2009).

1.3 Objectives

The objective of this exploratory study was to develop innovative anti-icing formulations for snow and ice control on highways by using beet sugar refining by-products and other bio-based additives. These formulations are expected to have improved ice-melting

and corrosion-inhibiting capacity with less impact on the durability of concrete and asphalt binder.

1.4 Expected Benefits

This project fits the research thrust of the Center for Environmentally Sustainable Transportation in Cold Climates (CESTiCC): *“reducing environmental impacts during construction, operations and preservation through effective design, management and preservation strategies.”* This project also meets the U.S. Department of Transportation’s (USDOT) strategic goal in environmental sustainability, as it helps *“advance environmentally sustainable policies and investments that reduce harmful emissions from transportation sources.”* Development of alternative anti-icing products serves the public interest. As such, research is expected to generate significant cost savings for DOTs and other maintenance agencies, traveler benefits in terms of improved safety and mobility, and societal benefits by *reducing the amount of chlorides in the environment.*



Figure 1.1 Sugar beets (left) and their harvesting in Montana (right)
(Courtesy: Montankids.com and BillingsGazette.com).

The findings from this work will provide maintenance agencies with more options in their snow and ice control toolbox for sustainable winter road service. The exploration of bio-based renewable additives for anti-icing applications will also add value to *agricultural by-products and stimulate local economies (e.g., the \$50+ million Montana beet sugar industry).*

CHAPTER 2.0 METHODOLOGY

2.1 Research Approach

The objective of this research was to develop anti-icing liquids consisting of cost-competitive chemicals (e.g., desugared beet molasses), rock salt, and other additives (e.g., bio-derived succinate salts, thickeners, concrete protection additives, and corrosion inhibitors). The optimized addition of renewable bio-based additives to salt brine enhances its anti-icing and deicing performance at cold temperatures, similar to the effect of $MgCl_2$, at reasonable costs, while producing substantial savings through reduced application rates, reduced corrosion to metals, and reduced impact on concrete or asphalt materials. The research team developed several liquid products tailored to meet the varying requirements in highway anti-icing performance, cost, and impacts. The team also addressed current gaps in the development of “green” anti-icers, that is, the synergy between various additives.

2.2 Work Plan – Task Descriptions and Milestones

2.2.1 Identify and Evaluate Individual “Green” Additives

The identification of “green” additives has mostly been built on the success of previous research by the principal investigator of this project. Patents and other published literature were also examined to understand recent research on the topic and identify active ingredients and additives for eco-friendly liquid formulations. This step is an essential part of a mass customization strategy that requires modular product design. The constituent materials selected should pose minimal toxicity to the environment (e.g., with low nitrogen, phosphate, and heavy metal contents), and those that come from eco-friendly cost-effective processes are preferred. Mixed with 23% salt brine, locally sourced bio-based materials (with or without further chemical treatment) and commercial additives with little toxicity were tested for their potential

in terms of improved ice-melting and corrosion-inhibiting capacity and reduced impact on asphalt binder and concrete material.

2.2.2 Statistical Design of Experiments

In order to minimize the number of experiments needed to explore a large domain of unknown factors and interactions, we used a scheme of statistical design of experiments known as uniform design (Fang et al., 2000). For instance, if we planned to investigate four influential factors, each varying at five different levels, without experimental design, there would be a total of $5^4 = 625$ experiments. With uniform design, however, we can choose to conduct only 30 experiments, the data from which should be sufficient to reasonably illustrate the inherent relations between the influential factors and the target factors.

Using uniform design, we chose four factors of X_1 , X_2 , X_3 , and X_4 as the weight percent of dandelion extract, sugar beet extract, sodium metasilicate, and sodium formate, respectively. The weight percent range of 0–3 was chosen for X_1 and X_2 , and 0–2 for X_3 and X_4 . Only sixteen anti-icer formulations were investigated by adopting the design parameters and associated target attributes, as shown in Table 2.1. There would be a total of $4 \times 4 \times 4 \times 4 = 256$ formulations to be investigated in the absence of a statistical design, as the dosage of all compounds varied at four levels.

2.2.3 Systematic Laboratory Investigation and Formulation Optimization

Following the established experimental design, several measures were used for screening tests of promising liquid formulations. To prepare the anti-icer formulations shown in Table 2.1, rock salt (taken from Washington State Department of Transportation), dandelion and sugar beet extracts, reagent-grade sodium metasilicate, and sodium formate and distilled deionized water were used. Each formulation had the same amount of rock salt (23 wt.%) and

various amounts of dandelion and sugar beet extracts, reagent-grade sodium metasilicate, and sodium formate, which were determined by using the uniform design table.

Table 2.1 Experimental design for anti-icer mixtures based on uniform design method.

Mix #	Weight percent of additives (%)			
	Dandelion extract	Sugar beet extract	Sodium metasilicate	Sodium formate
Mix 1	0	3	0	0.67
Mix 2	1	3	2	1.34
Mix 3	2	1	0	0
Mix 4	3	3	1.34	0
Mix 5	0	0	2	0
Mix 6	1	0	0	2
Mix 7	3	1	2	2
Mix 8	3	2	0	2
Mix 9	2	2	2	0.67
Mix 10	0	1	0.67	1.34
Mix 11	2	3	0.67	2
Mix 12	1	2	0.67	0
Mix 13	3	0	0.67	0.67
Mix 14	0	2	1.34	2
Mix 15	2	0	1.34	1.34
Mix 16	1	1	1.34	0.67

Preparation of the plant extract

For preparation of the plant extract, dandelions and sugar beets were collected, dried, and powdered. For preparing each extract, 30 g of the powder was chosen for chemical and biological degradation. For chemical degradation, 120 g urea and 0.5 g Ca(OH)₂ were first added to 200 mL deionized water. The dandelion powder and the sugar beet powder were added to this solution. The solution was stirred using a speed of 500 rpm for 30 min, during which 4 g NaOH was added to adjust the pH of the solution to around 11.6. The newly prepared solution was then placed in the refrigerator at -13°C. Once the freezing process started, the solution was

removed from the refrigerator and stirred uniformly with a stirring speed of 150 rpm for 30 min, during which 500 mL water was added. For biological degradation, the pH of the prepared solution was adjusted to around 8.5 by adding 15 mL HNO₃ and 6.5 g NaOH. A mixture of 1.274 g KH₂PO₄, 1.952 g NaH₂PO₄·H₂O, and 0.182 g MgSO₄·7H₂O was added to the solution to create an appropriate environment for the growth of bacteria. Next, 100 mL of *Bacillus megaterium* bacteria (NRRL B-14308) was added to the solution, and the solution was put in the shaker for 14 days to complete the biodegradation process.

Freeze-thaw test

The effects of anti-icers on concrete were assessed by conducting a freeze-thaw test of Portland cement mortar (PCM) samples in the presence of anti-icers, following the SHRP H205.8 test method with minor modifications. The test evaluates the combined effects of liquid chemicals and freeze-thaw cycling on the structural integrity of specimens of non-air-entrained mortar. Mortar samples were prepared in 5.1 cm × 10.2 cm (2 in.: diameter × 4 in.: length) poly (vinyl chloride) piping with a volume of 52.5 cm³. The mortar mix design had a water-to-cement ratio of 0:5, sand-to-cement ratio of 3:1, and water reducer of 1.5 mL. The cement used was Portland cement type I-II; the sand used was Sakrete multipurpose. Samples were cured in water for the first 24 h before being placed in a container with 100% relative humidity. The dry weight of each sample at 28 days was recorded before placing it on a sponge inside a dish containing 310 mL of diluted (3%) anti-icer solution. The dish was covered in plastic wrap to press the mortar samples into the sponge. Two mortar specimens were tested in each anti-icer solution. A 3 wt.% salt brine solution was used as the control. A thermocouple was embedded in one of the control mortar samples to monitor temperatures during freeze-thaw cycling. The sealed dishes were placed in the freezer for 16 to 18 h, at $-20.8 \pm 0.2^{\circ}\text{C}$ ($-5.44 \pm 0.4^{\circ}\text{F}$) followed by being placed in a laboratory environment at $23.2 \pm 0.2^{\circ}\text{C}$ ($73.8 \pm 0.4^{\circ}\text{F}$) for 6 to 8 h. The

cooling rate in the freezer and the heating rate in the laboratory environment were about $0.06^{\circ}\text{C}/\text{min}$ and $0.07^{\circ}\text{C}/\text{min}$, respectively. This cycle was repeated for 10 days. The test specimens were removed from the dish and rinsed under tap water to remove any scaled-off material. The specimens were air-dried overnight before the final weight of each was recorded.

Ice-melting test

The SHRP ice-melting test (H-205.1 and H-205.2) measures the amount of ice melted by deicers over time. In this test, liquid or solid deicers are uniformly spread over the prepared ice, and the melted liquid is removed for volume measurements (Chappelow et al., 1992). A modified SHRP test using 1.4 mL anti-icer, 48 mL distilled deionized water, and a 150×20 mm (5.9 in.: diameter \times 0.8 in.: depth) polystyrene petri dish was conducted to measure the ice-melting capacity of the anti-icer at -9.4°C (15°F). The anti-icer was applied evenly over the ice surface with a syringe. After 10, 20, 30, 45, and 60 min, the liquid volume was removed and volumetrically measured with a calibrated syringe. Another parallel series of tests were conducted in a $3.65 \text{ m} \times 4.27 \text{ m}$ state-of-the-art temperature-regulated environmental chamber, following the same procedure. The tests were conducted at -9.4°C (15°F) and -3.9°C (25°F). To ensure statistical reliability, triplicate tests were performed for each combination of deicer type and temperature.

Low-temperature behavior of asphalt binder

A customized test protocol was used to assess the effect of anti-icers on the low-temperature behavior of asphalt binder. A bending beam rheometer (BBR) was used for this purpose. Asphalt binder (PG 64-28 from Western States Asphalt, Inc.) was first aged in a rolling thin-film oven to simulate the effects of hot-mix asphalt concrete. The asphalt binder was then placed in a pressure aging vessel for 20 h to simulate 7–10 years of in-service aging. The asphalt binders were moved to a glass beaker, and 10 mL of anti-icer solution was applied

for each 30 g of binder, after which the beakers were put in a vacuum oven at 80°C for 1 h, followed by 2 h at 150°C at atmosphere pressure. Finally, beams were molded and tested in the BBR.

Ice-penetration test

Laboratory measurements of the ice penetration of various anti-icers were conducted following the SHRP H-205.4 test method. This test method measures the penetration behavior of liquid deicer on a cylinder of ice. The results of this test provide a measure of the penetration rate of the selected deicer over time. The test requires a custom-built Plexiglas[®] apparatus with holes drilled in it to form cavities. A section of 0.50 in. (1.3 cm) thick Plexiglas[®] 2 × 8 in. (5 × 20 cm) in size was drilled in order to form 10 cavities vertically along the margin of Plexiglas using a 5/32 in. (0.4 cm) drill bit to a depth of 3.5 cm, with 1.7 cm spacing between cavities. The cavities were enlarged at the top with a countersink bit to create a surface cone. These cavities were filled with deionized water and frozen for 12–24 h. Liquid deicer in the amount of 25 mL was dyed with 2 drops of food coloring (McCormick, red). The dyed liquid deicer solution was mixed and allowed to equilibrate to the given test temperature during freezing of the ice specimen. Three drops of dyed liquid deicer solution were pipetted onto the ice specimen. Often the penetration depth of dyed solutions was difficult to assess visually. When this occurred, to determine the penetration depth, a small metal probe was inserted in the cavity until it contacted the ice interface. The probe was maintained at the test temperature and did not contribute to any penetration or melting.

Corrosion behavior

The corrosion caused by anti-icers to C1010 carbon steel (ASTM A569) was assessed using the linear polarization resistance (LPR) technique. Measurements for this technique were carried out in a PARSTAT-MC multichannel potentiostat-galvanostat, coupled with a three-

electrode electrochemical cell for each channel. Before testing, the steel coupons were wet-polished using 60 to 1500 grit silicon carbide papers and washed with ethanol and distilled deionized water. For each anti-icer, 3 steel coupons were exposed to anti-icer for 24 h. The LPR measurement “is the only corrosion monitoring method that allows corrosion rates to be measured directly, in real time” (<http://www.alspi.com/lprintro.htm>). This electrochemical technique provides an alternative to the gravimetric method in rapidly assessing the corrosivity of solutions. The corrosivity of each anti-icer was reported as millinches per year (mpy).

Eutectic curves

To establish eutectic curves for anti-icer products, the test method standardized by ASTM International for automotive coolants (ASTM D1177 2012) was adopted. The test apparatus consisted of a plastic flask with deicer solution (100 mL), a stirrer made of stainless steel operated by wiper motor (60 to 80 stokes per minute), and a thermostat coupled with a data logger to measure temperature readings (for every second). The test apparatus was kept in a state-of-the-art temperature-regulated environmental chamber. The temperature of the chamber was reduced constantly until the deicer solution was frozen or supercooled. The cooling rate of the solution was approximately 0.5°C/min. According to the standard test protocol, “the freezing point is taken as the intersection of projections of the cooling curve and the freezing curve. If the solution supercools, the freezing point is the maximum temperature reached after supercooling” (ASTM D1177, 2012).

Chemical analysis

The chemical functional groups of the sugar beet by-product was obtained using Fourier transform infrared (FTIR) spectroscopy via a Nicolet 6700 FTIR spectrometer (Thermo Fisher

Scientific, Madison, WI). The infrared (IR) spectra of the samples were collected over the wave number range of 4000 to 400 cm^{-1} .

The liquid chromatography–mass spectrometry (LC-MS) technique was used for more accurate chemical analysis of sugar beet extract. First, 135 mg of dried beet extract was reconstituted in 1 mL 50% aqueous methanol; then the debris was removed by centrifugation for 10 min. The resulting supernatant was filtered through a 0.2 μm Acrodisc filter. Of the resulting extracts, 3 μL were loaded onto a 50 \times 2.1 mm Acquity BEH C18 column (Waters) and eluted using a linear gradient of acetonitrile-water containing 0.1% formic acid at a flow rate of 0.4 mL/min. The analysis was conducted in positive ion mode using Synapt G2-S (Waters), a quadrupole time-of-flight mass spectrometer. The capillary was at 3 kV, the source temperature was at 120°C, and the desolvation gas flow was at 850 L/h. The data collected were corrected using the signal of the co-infused reference compound leucine enkephaline.

Friction test

In general, techniques and equipment used to measure friction in the laboratory tend to look and operate much differently than devices used in the field. While some standardized equipment is available, several friction measuring devices have been custom designed and built for specific research projects. Simple devices usually include a metal block with a rubber pad on the bottom that is pulled across the surface. The ratio of the force needed to pull the block (initiate movement) divided by the weight of the block is the coefficient of static friction. The aforementioned method was used in this research.

Note that the Montana State University (MSU) research team submitted a separate proposal to CESTiCC that included one task to support the Washington State University (WSU) research. Specifically, the MSU team evaluated two liquid anti-icing formulations developed by the WSU research team, using 23 wt.% NaCl as the control. The evaluation entailed SHRP

ice-melting and SHRP ice-penetration test methods at two select temperatures (e.g., 15°F and 25°F). One viable formula (“best performer”) was tested for freezing point depression phase diagram (ASTM D1177-88) and the friction coefficient of asphalt pavement treated by this anti-icing formulation (vs. 23wt.% NaCl) at a certain temperature near 25°F or 30°F after being applied at 30 gal per lane mile (1 hour after simulated trafficking and plowing).

CHAPTER 3.0 RESULTS AND DISCUSSION

3.1 Ice-Melting Capacity of Anti-icers

Figure 3.1 shows the 60 min ice-melting capacity of selected anti-icers at 15°F. The differences in ice-melting capacity between salt brine and mixtures 3, 6, 9, 10, and 12–16 were relatively small (less than 0.3 mL brine/g anti-icer), which indicates no or low advantage of their use over salt brine. Samples 1, 2, 4, 5, 7, 8, and 11 had an ice-melting capacity of at least 0.3 unit more than salt brine, which made them potential candidates for the final choice in terms of ice-melting performance.

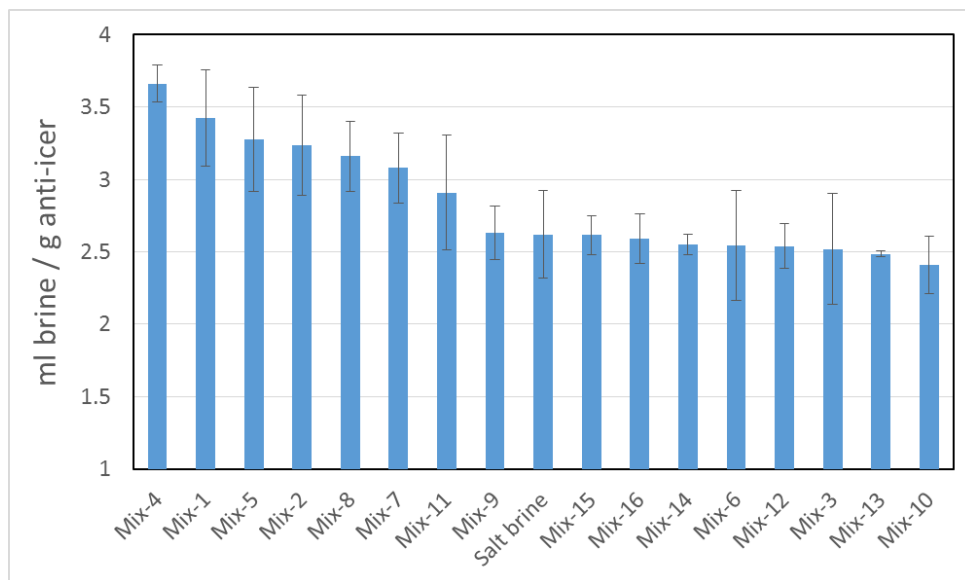


Figure 3.1 Ranking of mixtures based on ice-melting capacity after application of anti-icers at 60 min, 15°F obtained using a SHRP test method.

3.2 Freeze-Thaw Resistance of PCM in the Presence of Anti-icers

The presence of anti-icers generally degraded the freeze-thaw resistance of PCM. In this test program of various anti-icers, salt rock was the control. Using the non-air-entrained PCM samples, salt rock caused approximately 1.5% weight loss after 10-day cycles of SHRP freeze-thaw testing. Among the anti-icers tested, Mix 11 caused the most weight loss of the mortar sample (about 2.3%), followed by Mix 13 and Mix 14 (approximately 2.2%), whereas

Mix 2 and Mix 1 caused weight gains of 0.13% and 0.008%, respectively (as shown in Figure 3.2). The weight gains could be due to the adsorption of anti-icers, since notable scaling was found with the PCM samples exposed to Mix 2 and Mix 1.

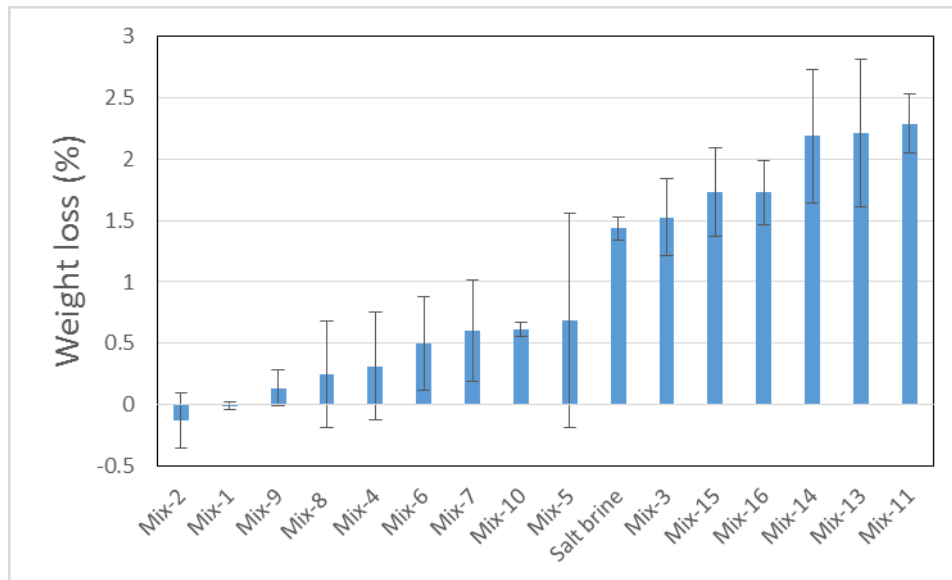


Figure 3.2 Weight loss of Portland cement mortars exposed to various anti-deicer mixtures after the 10-day SHRP H205.8 freeze-thaw test

3.3 Effect of Freeze-Thaw in the Presence of Anti-icers on PCM Strength

Figure 3.3 illustrates the average compressive strength of PCM samples after 10-cycle freeze-thaw testing in various anti-icers, along with a control sample in salt brine. A comparison of Figure 3.2 and Figure 3.3 shows there is no direct relationship between the weight loss results and the compression test results. For instance, samples exposed to Mix 2 had the least weight loss, but the maximum compression strength is observed for specimens exposed to Mix 5. These results implied the significant beneficial effect of silicate and the moderate role of formate on the compression strength of PCM samples.

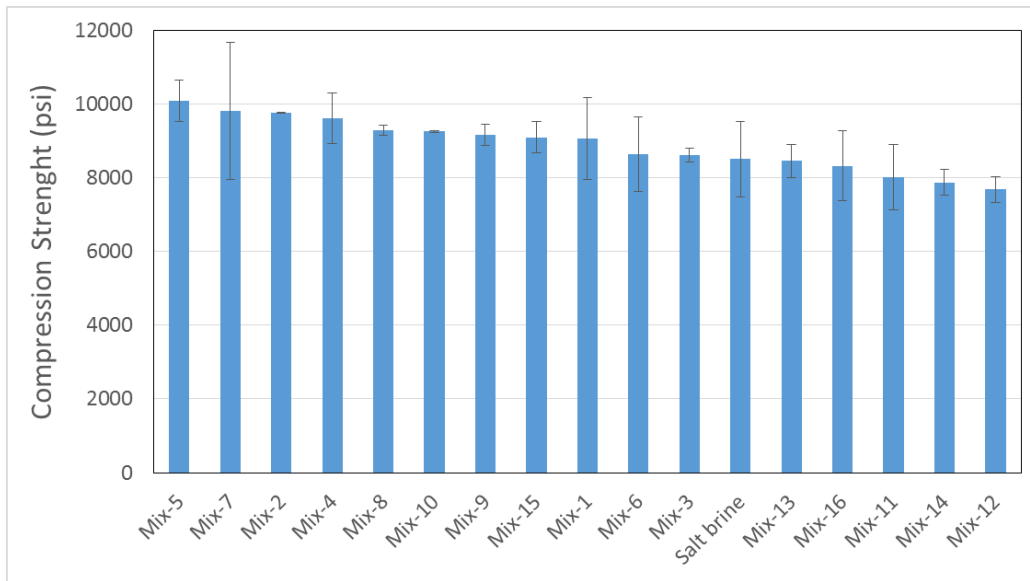


Figure 3.3 Compressive strength of mortar as a function of anti-icer type after 10-cycle freeze-thaw test.

3.4 Impacts of Anti-icer Mixtures on Asphalt Pavements

The effect of anti-icers on asphalt was assessed with a bending beam rheometer (BBR) by exposing the asphalt binder to anti-icers, thermal and pressure aging, and subsequent testing of the binder beams with the BBR. The BBR test provides values for creep stiffness and m -value (Figure 3.4 and Figure 3.5). Higher stiffness values correspond to higher thermal stresses, so a maximum limit of about 136.93 MPa was specified. On the other hand, lower m -values indicate less ability to relax, so a minimum limit of about 0.307 was specified. The m -value and stiffness values varied, in the range of 0.307–0.362 MPa and 74.24–136.93 MPa, respectively. The experimental results indicated a moderate impact of anti-icer design on the performance of asphalt binder. The negative effect of some anti-icer mixtures on asphalt performance by increasing its creep stiffness value can be due to the binder emulsification (Shi et al., 2009a).

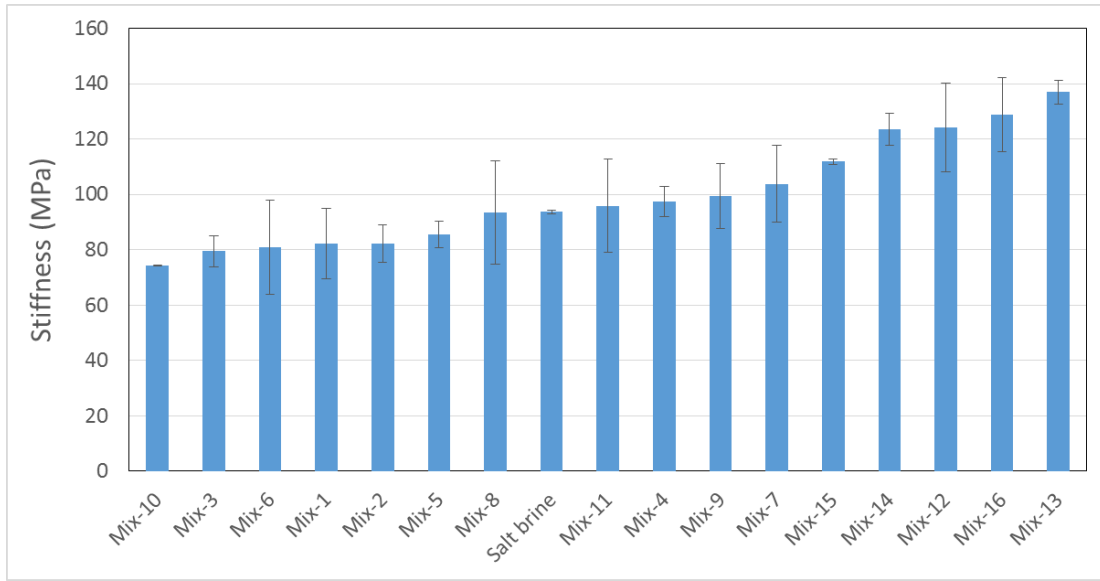


Figure 3.4 The stiffness of asphalt binder exposed to various anti-icer mixtures obtained by a BBR.

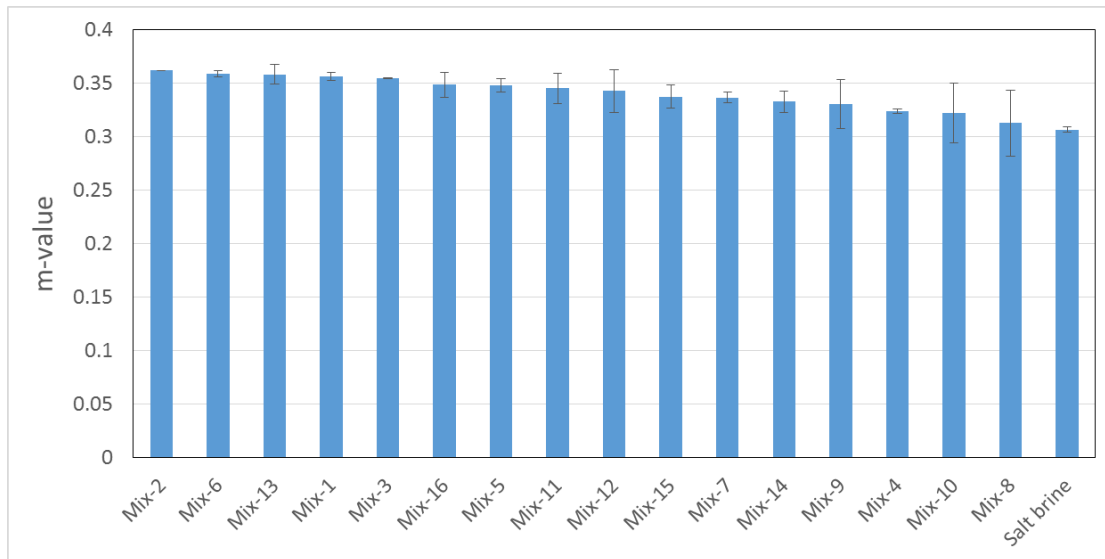


Figure 3.5 The *m*-value of asphalt binder exposed to various anti-icer mixtures obtained by a BBR.

3.5 The Corrosivity of Anti-icer Mixtures on Mild Steel

As shown in Figure Figure 3.6, the mixtures containing sodium metasilicate were the least corrosive to C1010 carbon steel samples, with corrosion rates of equal to or less than 0.107 mpy (mils/milliinches per year), whereas the mixtures containing only bio-derived

extracts (Mix 3) and those containing both bio-derived extracts and sodium formate (Mix 8, Mix 6, Mix 1) were considered the most corrosive. However, the corrosivity of later mixtures was still much less than the corrosivity of salt brine. For instance the corrosion inhibition efficiency of Mix 1, which was calculated using Equation 3.1, is 36.45%.

$$IE\% = \left(\frac{CR_{uninhibited} - CR_{inhibited}}{CR_{uninhibited}} \right) \times 100 \quad (3.1)$$

where IE is inhibition efficiency, and $CR_{uninhibited}$ and $CR_{inhibited}$ are the corrosion rates of the mild steel samples exposed to salt brine and to anti-icer mixtures, respectively.

Note that the patterns of anti-icer corrosion to C1010 carbon steel apparently contradicted the users' perspective. No conclusions can be drawn without considering the ice-melting capacity of the anti-icer mixtures and their impacts on mortar and asphalt. In particular, ice-melting capacity is the most important factor influencing the selection of the best performer anti-icer mixture.

3.6 FTIR Spectroscopy of Sugar Beet By-product

Fourier transform infrared (FTIR) spectroscopy is an analytical technique that measures the infrared intensity versus wavelength—wave number (cm^{-1})—of light. Infrared spectroscopy detects the vibration characteristics of chemical functional groups in a sample as the groups stretch, contract, and bend when exposed to infrared light. As a result, a chemical functional group adsorbs infrared radiation in a specific wave number range regardless of the structure of the rest of the molecule, the effect of temperature, and the pressure, sampling, or change in the molecular structure in other parts of the molecules. Therefore the presence of specific functional groups can be monitored by signals in certain wave number ranges (Shi et al., 2009b).

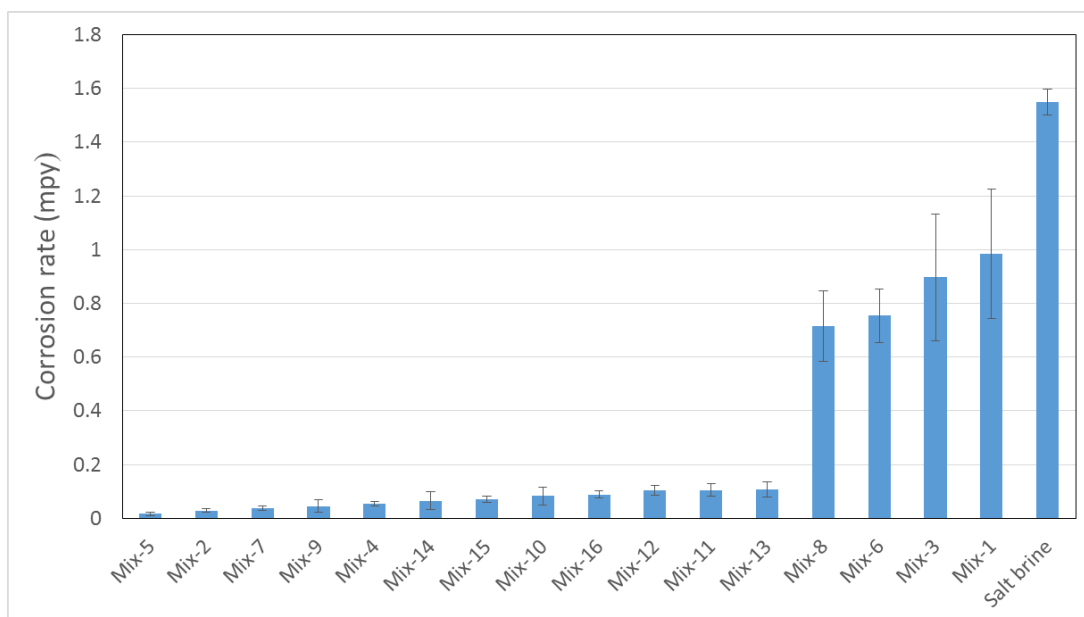


Figure 3.6 Corrosivity of the anti-icer mixtures on C1010 carbon steel after 24 h immersion measured by LPR.

The sugar beet by-product was characterized using FTIR spectra (Figure 3.7). The functional groups identified from Figure 3.7 are presented in Table 3.1 Two peaks that appear at 3421 and 3324 cm^{-1} are attributed to primary and secondary amines. Amines are well-known corrosion inhibitors, especially in salt brine. Amines can protect carbon steel in salt brine by forming an adsorbed barrier layer on the surface carbon steel, which follows the Langmuir adsorption isotherm (Alsabagh et al., 2006). A small peak that appears at 2157 cm^{-1} could be attributed to alkynes groups. The peak at 1668 cm^{-1} indicates the presence of alkenes. The absorption bands observed at 1583 and 1153 cm^{-1} are due to primary amines and aliphatic amines, respectively. A peak at 1456 cm^{-1} is attributed to alkanes, and the peak at 555 cm^{-1} is due to alkyl halides. The source of alkyl halides could be the bacterial culture media that contains protein and thus halides (Carugo, 2014).

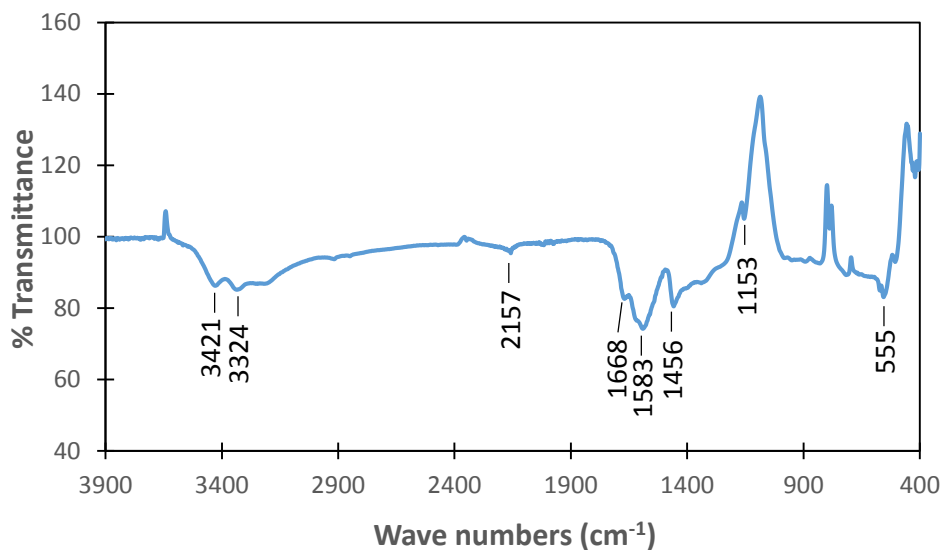


Figure 3.7 FTIR spectra for sugar beet by-product.

Table 3.1 Chemical functional groups of the sugar beet by-product obtained using FTIR spectroscopy.

Wave number (cm ⁻¹)	Functional group	Bond	Frequency range (cm ⁻¹)
3421 and 3324	1°, 2° amines	N–H Stretch	3400–3250
2157	alkynes	–C≡C– stretch	2260–2100
1668	alkenes	–C=C– stretch	1680–1640
1583	1° amines	N–H bend	1650–1580
1456	alkanes	C–H bend	1470–1450
1153	aliphatic amines	C–N stretch	1250–1020
555	alkyl halides	C–Cl stretch	850–550

3.7 Liquid Chromatography–Mass Spectrometry

The results of the liquid chromatography-mass spectrometry (LC-MS) of the sugar beet by-product are presented in Figure 3.8 and Table 3.2; they are in good agreement with the FTIR results. According to the mass spectrum data, the sugar beet by-product contains oxygen, nitrogen, phosphorus, and sulfur. The organic compounds containing O, N, S, and P have a polar function such that they can be adsorbed on the surface of metal and reduce the corrosion rate by blocking active corrosion sites (Dariva and Galio, 2014).

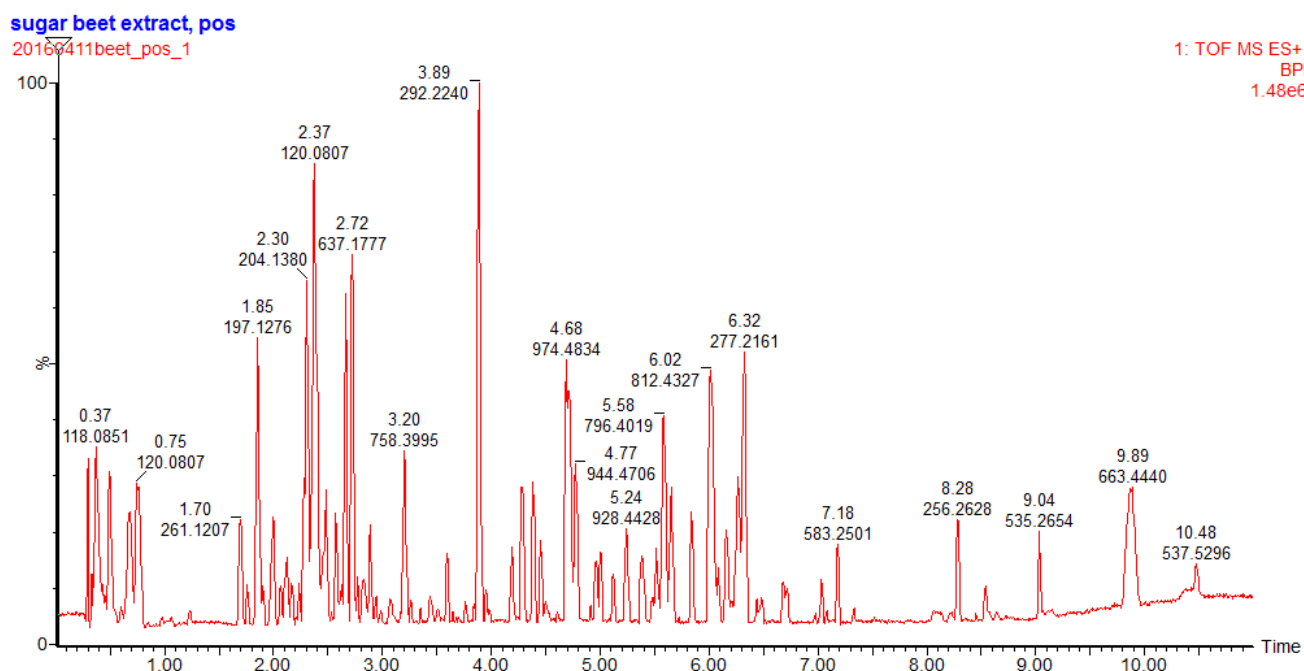


Figure 3.8 LC-MS spectra of sugar beet extract.

Table 3.2 Summary of the chemical constituents detected for sugar beet by-product using the liquid chromatography-mass spectrometry (LC-MS) technique.

Formula	m/z
$C_{41}H_{71}N_{11}O_{14}S$	974.4974
$C_{42}H_{63}O_4P$	663.4538
$C_{27}H_{30}F_2N_6O_8S$	637.1888
$C_{18}H_{29}NO_2$	292.2282
$C_{15}H_{12}N_{6+2}$	277.1187
$C_{11}H_{12}N_2O_2$	205.0968
$C_{10}H_{16}N_2O_2$	197.1283
C_9H_{12}	121.1012

3.8 Complementary Tests

The MSU research team submitted a separate proposal to CESTiCC that included one task that supported the WSU research. Specifically, the MSU team evaluated two liquid anti-icing formulations developed by the WSU team, using 23 wt.% NaCl as the control. The evaluation entailed the SHRP ice-melting and SHRP ice-penetration test methods at two select

temperatures (e.g., 15°F and 25°F). One viable formula (“best performer”) was tested for freezing point depression phase diagram (ASTM D 1177-88) and the friction coefficient of asphalt pavement treated by this anti-icing formulation (vs. 23 wt.% NaCl) at a certain temperature near 25°F or 30°F after being applied at 30 gal per lane mile (1 hour after simulated trafficking and plowing).

3.8.1 Ice-Melting Capacity of Selected Anti-icers

The ice-melting capacity of the selected anti-icers varied as a function of product type and test temperature. At 25°F, Mix 1 had a relatively high ice-melting capacity over time especially between 30 min to 60 min after the test started (Figure 3.9). However, the salt brine performed better than the selected liquid deicer products at 15°F (Figure 3.10). At 15°F, all the anti-icer formulations exhibited less ice-melting capacity than at 25°F. The difference between the test results reported in this section and the results obtained by the WSU research team (reported in Section 3.1) may be attributed to a difference in the detailed test protocol and the use of a state-of-the-art environmental chamber by the MSU team for running the ice-melting test.

3.8.2 Ice-Penetration Rate of Selected Anti-icers

The ice-penetration capability of the selected anti-icers also varied as a function of product type and test temperature. Overall, salt brine outperformed both Mix 1 and Mix 5 at 25°F and 15°F (Figure 3.11 and Figure 3.12). At 25°F, the mixtures showed better ice-penetration performance than salt brine until 30 min. After 30 min, the ice-penetration performance of salt brine exceeded that of mixtures. Note that the penetration performance for all deicers gradually diminished as the temperature grew colder.

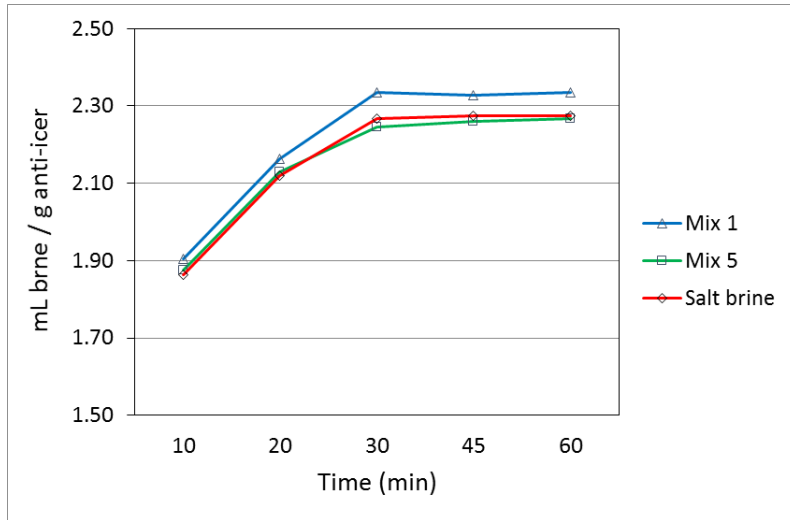


Figure 3.9 Ice-melting capacity as a function of time at 25°F obtained using the SHRP test method.

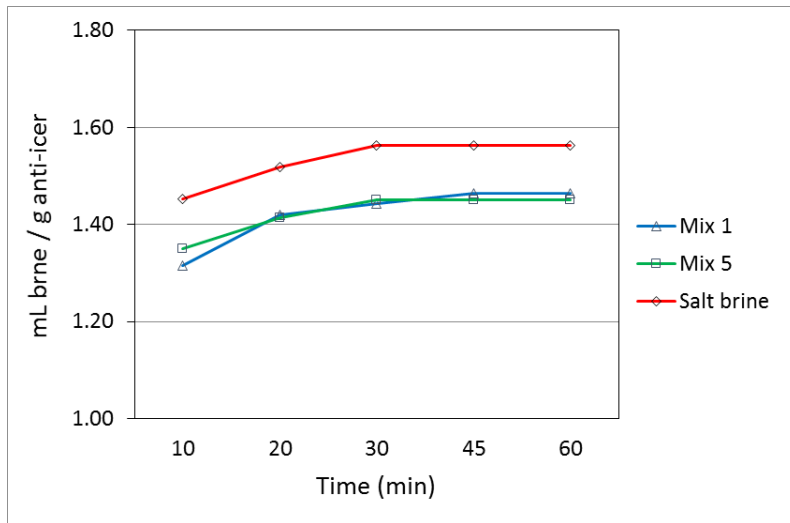


Figure 3.10 Ice-melting capacity as a function of time at 15°F obtained using the SHRP test method.

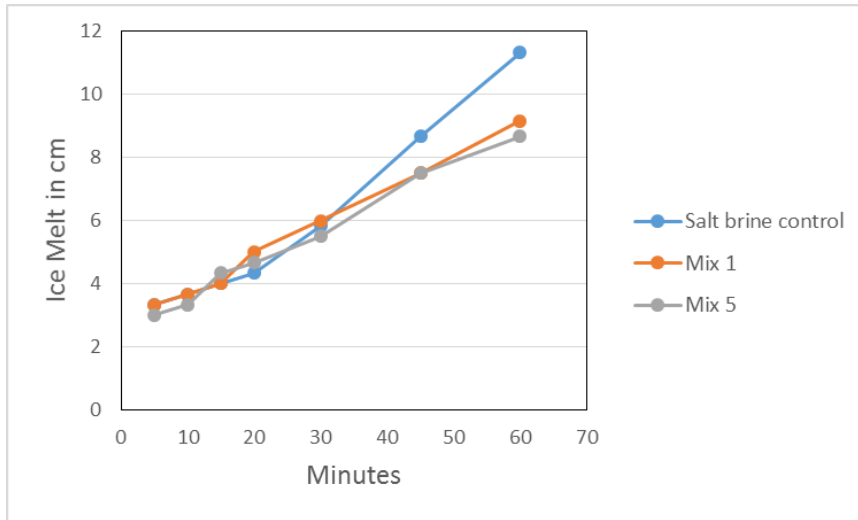


Figure 3.11 Ice-penetration rate as a function of time at 25°F obtained using the SHRP test method.

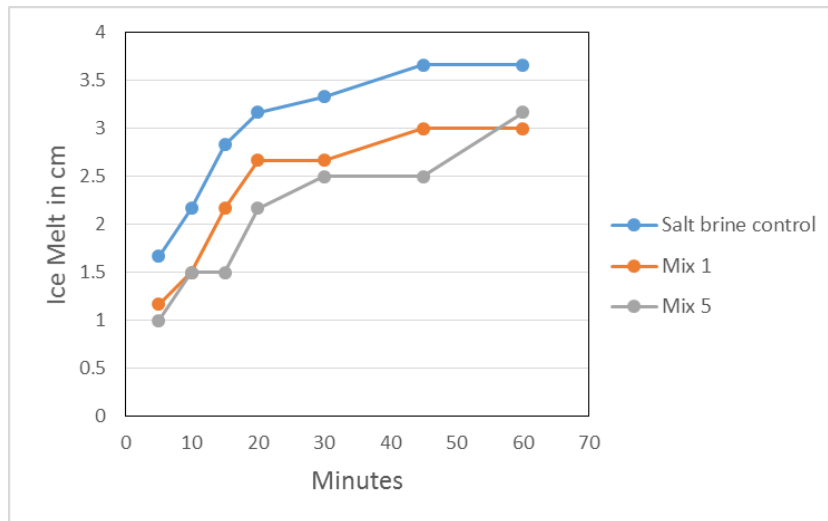


Figure 3.12 Ice-penetration rate as a function of time at 15°F obtained using the SHRP test method.

3.8.3 Eutectic and Effective Temperatures

A eutectic curve illustrates the freezing point temperature of an aqueous solution as a function of its concentration. At the eutectic point, there exists equilibrium between ice, salt, and a solution with a specific concentration. This specific concentration is called the eutectic concentration, and the corresponding temperature at this equilibrium is called the eutectic

temperature. In the case of anti-icer solutions, eutectic temperature is the minimum temperature at which an anti-icer solution remains in liquid form. Above the eutectic concentration, the excess anti-icing chemicals crystallize due to the saturation of liquid. In other words, the freezing point of the solution decreases with increasing concentration up to the eutectic concentration (Koefod, 2009). As shown in Figure 3.13, the lowest freezing point (i.e., the eutectic temperature) for salt brine is -22.78°C (-9°F) at a concentration of 23 wt.%; for Mix 1, it was -15.7°C (3.74°F) at a concentration of 25 wt.%. The lower eutectic temperature of Mix 1 relative to the salt brine indicated that thermodynamically, Mix 1 is more powerful than salt brine.

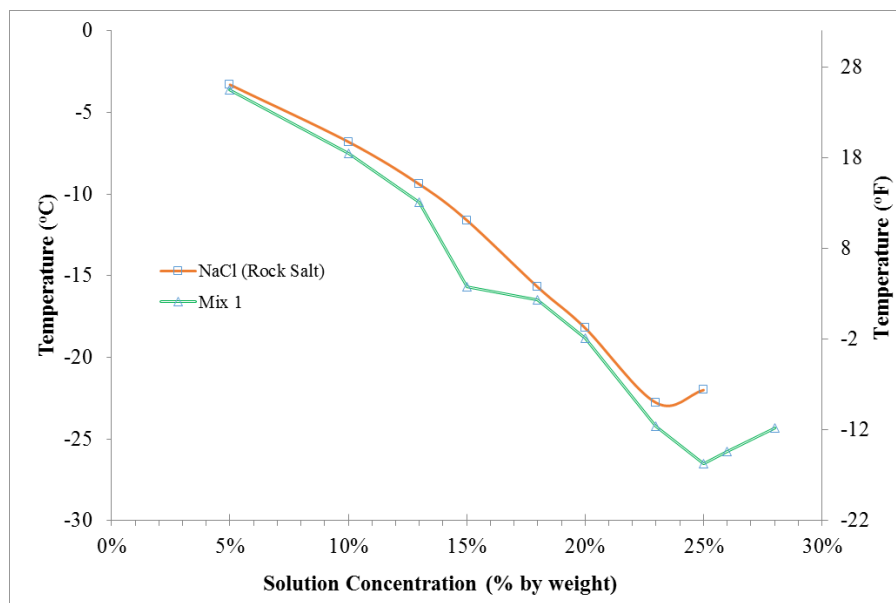


Figure 3.13 Eutectic curves of salt brine and Mix 1.

3.8.4 Friction Coefficient of Anti-iced Pavement Surface

In comparison with using salt brine, the application of Mix 1 resulted in a pronouncedly improved effect on the friction coefficient, according to the laboratory measured friction coefficients of the anti-iced pavement after plowing (Figure 3.14). This improved effect suggests that the agro-based materials used in the composition of Mix 1 reduce the slipperiness

of anti-iced pavement better than salt brine. The reason for this improvement in friction coefficient can be the better performance of Mix 1 in terms of ice melting, ice penetration, and possibly ice undercutting, relative to salt brine. Or it could be related to an increase in actual contact area (Waluś and Olszewski, 2011) due to the cellulosic structure of the agro-based materials used in the formulation of Mix 1.

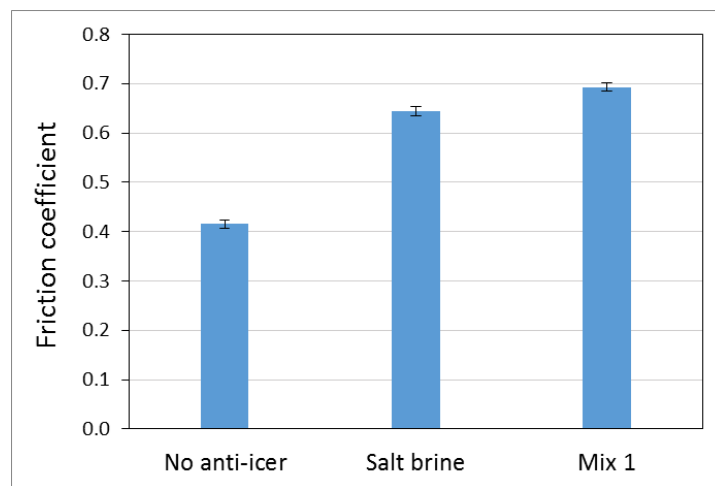


Figure 3.14 Friction coefficient on the iced asphalt pavement at about 25°F in the absence of anti-icer and after application of salt brine and Mix 1 as anti-icers.

CHAPTER 4.0 CONCLUSIONS AND RECOMMENDATIONS

This report describes the performance and impact of a group of 16 anti-icer mixtures that were designed based on the previous experiences of the authors, using the uniform design method. Selected constituent materials pose minimal toxicity to the environment (e.g., no heavy metal contents) and were derived from eco-friendly, cost-effective processes. Bio-based solutions derived from locally sourced agro-based materials mixed with 23 wt.% salt brine, and commercial additives (with little toxicity) were tested for their ice-melting capacity, ice-penetration rate, ability to protect asphalt binder and concrete, effect on the friction coefficient of iced asphalt pavement, and anti-corrosion performance. A 23 wt.% salt brine was considered the control. The main criteria for choosing the best performing anti-icer were ice-melting capacity and capability to increase the friction coefficient of the iced asphalt pavement. For instance, Mix 1 which is a water-based solution made of **3 wt.% sugar beet extract, 0.67 wt.% sodium metasilicate, and 23 wt.% sodium chloride** was chosen as the best performing anti-icer despite its less-than-ideal anticorrosion property compared with the rest of the “green” anti-icer mixtures. This decision came from its high ice-melting capacity and its high capability to increase the friction coefficient of the iced asphalt pavement at 25°F. The enhanced snow/ice control performance of Mix 1 may translate to a reduced application rate required on pavement. In addition, Mix 1 had a good ice-penetration rate and had low impact on Portland cement mortar in terms of scaling, based on results from the 10-cycle freeze-thaw test. The mortar samples exposed to Mix 1 during the 10-cycle freeze-thaw test showed moderate compression strength. Mix 1 also had little impact on asphalt binder and showed less corrosivity relative to conventional salt brine. This research contributes to the knowledge base relevant to bio-based anti-icers and introduces a new class of high-performance “green” anti-icers. Before scale-up production of these materials, more research is necessary to optimize the formula and field

validate its performance. Future research could include the exploration of other types of “greener” anti-icers consisting of additives derived from renewable resources other than sugar beet.

CHAPTER 5.0 REFERENCES

- Alsabagh, A. M., Migahed, M. A., and Awad, H. S. (2006). "Reactivity of polyester aliphatic amine surfactants as corrosion inhibitors for carbon steel in formation water (deep well water)." *Corros. Sci.*, 48, 813–828.
- ASTM D1177. (2012). "Standard test method for freezing point of aqueous engine coolants." ASTM International.
- Bloomer, T. A. (2002). "Anti-freezing and deicing composition and method." US6416684 B1.
- Carugo, O. (2014). "Buried chloride stereochemistry in the protein data bank." *BMC Struct. Biol.*, 14(19), 10.1186/s12900-014-0019-8.
- Chappelow, C. C., McElroy, A. D., Blackburn, R. R., Darwin, D., and Locke, C. E. (1992). *Handbook of test methods for evaluating chemical deicers*. Strategic Highway Research Program, National Research Council, National Academy of Sciences, Washington DC.
- Conger, S. M. (2005). "Winter highway operations." *NCHRP Synthesis 344*. Transportation Research Board, Washington, DC.
- Dariva, C. G., Galio, A. F. (2014). "Corrosion inhibitors – principles, mechanisms and applications." in: Aliofkhazraei, M. (Ed.), *Developments in corrosion protection*. InTech.
- Fang, K. -T., Lin, D. K. J., Winker, P., and Zhang, Y. (2000). "Uniform design: Theory and application." *Technometrics*, 42, 237–248.
- Fay, L., Jungwirth, S., Li, Y., and Shi, X. (2014). "Toxicological effects of chloride-based deicers in the natural environment: Synthesis of existing research." *Proc.*,

- Transportation Research Board 93rd Annual Meeting*, Transportation Research Board Washington, DC, paper # 14-4017.
- Fay, L., Shi, X., and Huang, J. (2013). "Strategies to mitigate the impacts of chloride roadway deicers on the natural environment." *NCHRP Synthesis 449*. Transportation Research Board, Washington, DC.
- Kelly, V. R., Findlay, S. E. G., Schlesinger, W. H., Menking, K., and Chatrchyan, A. M. (2010). "Road salt: Moving toward the solution." *Special Report*. The Cary Institute of Ecosystem Studies.
- Koefod, S. (2009). "A better understanding of chemical deicing: Facts and myths." *APWA 2009 Congress*, Columbus, Ohio.
- Li, Y., Fang, Y., Seeley, N., Jungwirth, S., Jackson, E., and Shi, X. (2013). "Corrosion by chloride deicers on highway maintenance equipment: Renewed perspective and laboratory investigation." *Transp. Res. Rec. J. Transp. Res. Board*, 2361, 106–113.
- Ossian, K. C., and Behrens, K. (2009). "Processed raffinate material for enhancing melt value of de-icers." US7473379 B2.
- Sapienza, R., Johnson, A., and Ricks, W. (2012). "Environmentally benign anti-icing or deicing fluids." US8241520 B2.
- Sapienza, R., Johnson, A., and Ricks, W. (2005). "Environmentally benign anti-icing or deicing fluids employing triglyceride processing by-products." US6890451 B2.
- Shi, X., Akin, M., Pan, T., Fay, L., Liu, Y., and Yang, Z. (2009a). "Deicer impacts on pavement materials: Introduction and recent developments." *Open Civ. Eng. J.*, 3, 16–27.
- Shi, X., Fay, L., Gallaway, C., Volkening, K., Peterson, M. M., Pan, T., Creighton, A., Lawlor, C., Mumma, S., Liu, Y., and Nguyen, T. A. (2009b.) "Evaluation of alternate

anti-icing and deicing compounds using sodium chloride and magnesium chloride as baseline deicers." *Final Report No. CDOT-2009-1*. Colorado Department of Transportation.

Shi, X., Veneziano, D., Xie, N., and Gong, J. (2013). "Use of chloride-based ice control products for sustainable winter maintenance: A balanced perspective." *Cold Reg. Sci. Technol.*, 86, 104–112.

Staples, J.M., Gamradt, L., Stein, O., and Shi, X. (2004). "Recommendation for winter traction materials management on roadways adjacent to bodies of water." *Report No. FHWA/MT-04-008/8117-19*. Montana Department of Transportation, Helena, MT.

Taylor, P., Verkade, J., Gopalakrishnan, K., Wadhwa, K., and Kim, S. (2010). "Development of an improved agricultural-based deicing product." *Final Report*. Institute for Transportation, Iowa State University.

Waluś, K.J., and Olszewski, Z. (2011). "Analysis of tire-road contact under winter conditions." *Proc., the World Congress on Engineering (WCE) 2011*, London, U.K.

Ye, Z., Strong, C., Fay, L., and Shi, X. (2009). "Cost benefits of weather information for winter road maintenance." *Final Report*. Iowa Department of Transportation.

APPENDIX A

Figures A.1–A.17 are pictures of concrete samples after they had been soaked in different anti-icer solutions during a 10-cycle freeze-thaw test to see the effects of the various anti-icer solutions on concrete.



Figure A.1 Mix 1 was used for samples 1 and 2.

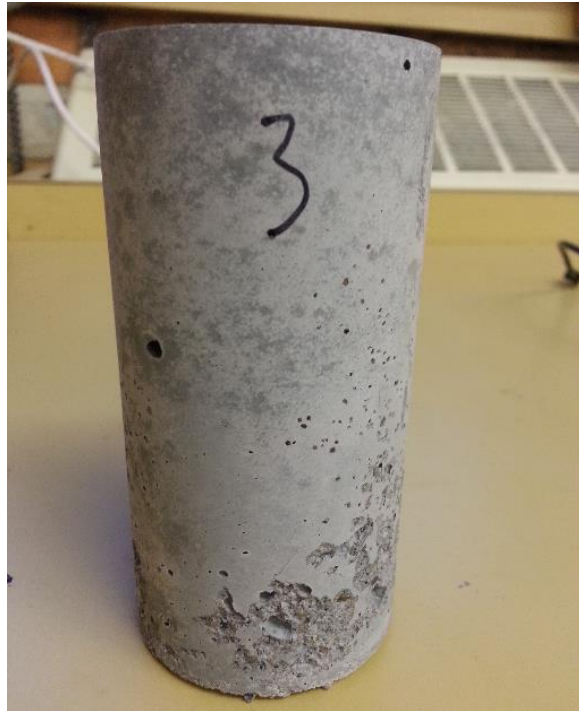


Figure A.2 Mix 2 was used for samples 3 and 4.



Figure A.3 Mix 3 was used for samples 5 and 6.



Figure A.4 Mix 4 was used for samples 7 and 8.



Figure A.5 Mix 5 was used for samples 9 and 10.



Figure A.6 Mix 6 was used for samples 11 and 12.

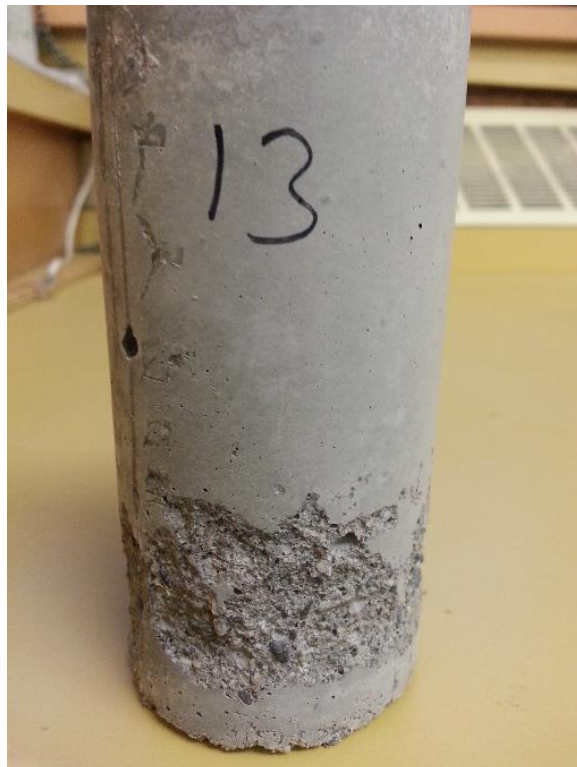


Figure A.7 Mix 7 was used for samples 13 and 14.



Figure A.8 Mix 8 was used for samples 15 and 16.



Figure A.9 Mix 9 was used for samples 17 and 18.



Figure A.10 Mix 10 was used for samples 19 and 20.



Figure A.11 Mix 11 was used for samples 21 and 22.

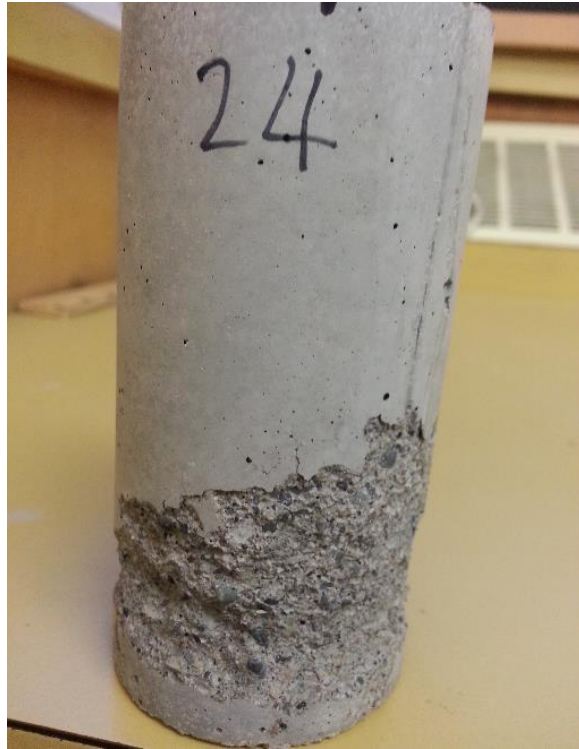


Figure A.12 Mix 12 was used for samples 23 and 24.



Figure A.13 Mix 13 was used for samples 25 and 26.



Figure A.14 Mix 14 was used for samples 27 and 28.

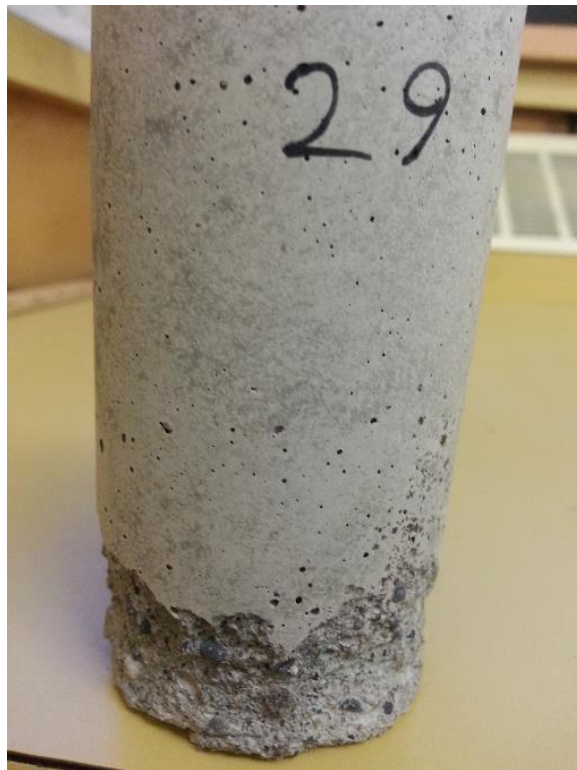


Figure A.15 Mix 15 was used for samples 29 and 30.



Figure A.16 Mix 16 was used for samples 31 and 32.

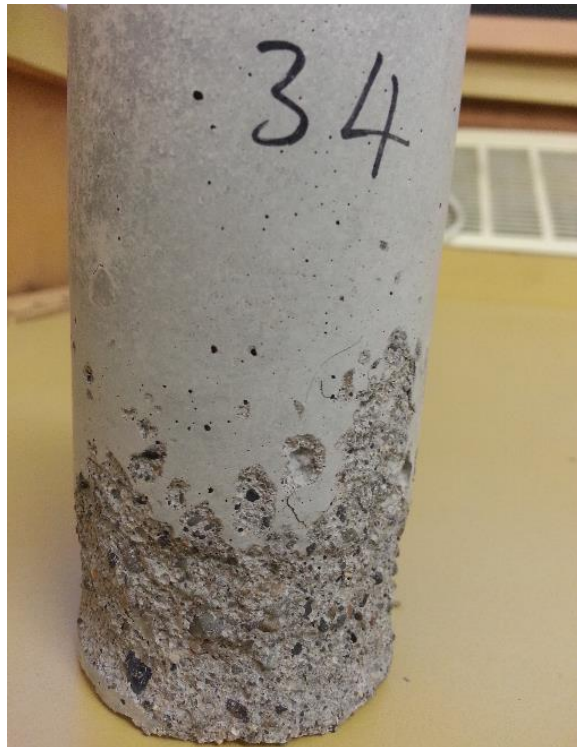


Figure A.17 Salt brine was used for samples 33 and 34.